Available online at www.sciencedirect.com
ScienceDirect
Journal of Nuclear Materials 371 (2007) 18–27
journal of nuclear materials
www.elsevier.com/locate/jnucmat

# The effect of neutron irradiation damage on the properties of grade NBG-10 graphite

Timothy D. Burchell *, Lance L. Snead

*Materials Science and Technology Division, Oak Ridge National Laboratory, P.O. Box 2008, Oak Ridge, TN 37831-6088, USA*

**Abstract**

Nuclear block graphite-10 (NBG-10) is a medium-grain, near-isotropic graphite manufactured by SGL Carbon Company at their plant in Chedde, France. NBG-10 graphite was developed as a candidate core structural material for the pebble bed modular reactor (PBMR) currently being designed in South Africa, and for prismatic reactor concepts being developed in the USA and Europe. NBG-10 is one of several graphites included in the US-DOE Very High Temperature Reactor (VHTR) program. Thirty-six NBG-10 graphite flexure bars have been successfully irradiated in a series of 18 HFIR PTT capsules at ORNL. The capsule irradiation temperatures were $294 \pm 25$, $360 \pm 25$ and $691 \pm 25$ °C. The peak doses attained were 4.93, 6.67, and $6.69 \times 10^{25}$ n/m$^2$ [$E > 0.1$ MeV] at ~294, ~360, and ~691 °C, respectively. The high temperature irradiation volume and dimensional change behavior, and flexure strength and elastic modulus changes of NBG-10 were similar to other extruded, near-isotropic grades, such as H-451, which has been irradiated previously at ORNL. The low temperature (~294 °C) irradiation volume and dimensional change behavior was also as expected for extruded graphites, i.e., exhibiting low dose swelling prior to shrinkage. This behavior was attributed to the relaxation of internal stress arising from the graphite manufacturing process and specimen machining. While the data reported here do not represent a complete database for NBG-10 graphite, they give a measure of confidence that the current generation of nuclear graphites will behave in a familiar and well understood manner.
Published by Elsevier B.V.

## 1. Introduction

Nuclear block graphite-10 (NBG-10) is a medium-grain, near-isotropic graphite manufactured by SGL Carbon Company at their plant in Chedde, France. The filler coke is coal tar pitch derived (maximum size ~1.6 mm). The graphite is formed by extrusion and doubly impregnated. The formulation and manufacturing process are based on that of the graphite fuel sleeves used for advanced gas cooled reactor fuel stringers in the United Kingdom. NBG-10 graphite was developed as a candidate core structural material for the pebble bed modular reactor (PBMR) currently being designed in South Africa, and for prismatic reactor concepts being developed in the USA and Europe. NBG-10 is one of several graphites included in the United States Department of Energy Very High Temperature Reactor program.

## 2. Experimental

Flexural bars were irradiated in the target region of the high flux isotope reactor (HFIR) at Oak

* Corresponding author. Fax: +1 865 576 8424.
*E-mail address:* burchelltd@ornl.gov (T.D. Burchell).

0022-3115/$ - see front matter Published by Elsevier B.V.
doi:10.1016/j.jnucmat.2007.05.021

Ridge National Laboratory (ORNL) in the peripheral target tube (PTT) positions. A total of 18 irradiation capsules, each containing two bend bars, were filled with static ultra high purity helium, neon, or argon depending on the target temperature required. Each bend bar was approximately $3.18 \times 6.35 \times 50.8$ mm. Capsules were irradiated in a range of core axial positions of variable fast neutron flux. The range in flux was from 3.7 to $9.9 \times 10^{18}$ n/m$^2$ s ($E > 0.1$ MeV). Each bend bar had a Rohm Haas high purity chemical vapor deposited silicon carbide (SiC) 'temperature monitor' pressed to its surface using a spring. These monitors were read using an isochronal annealing and electrical resistivity technique as described elsewhere [1]. The measured irradiation temperatures were $294 \pm 25$, $360 \pm 25$ and $691 \pm 25$ °C.

Dimensions and mass of all flexural bars were measured before and after neutron irradiation using certified, calibrated equipment. Mechanical properties were evaluated by four-point flexural testing at ambient temperature for both irradiated specimens and non-irradiated specimens according to ASTM C1341-00. The support span and the loading span were 40 and 20 mm, respectively. The crosshead speed was 8.5 μm/s. The crosshead displacement was used to determine the specimen deflection. Dynamic elastic modulus was also measured on all specimens before and after irradiation by impulse excitation and vibration method following ASTM C1259-01. Dynamic modulus was measured using excitation along the bar length from both the width and thickness orientations. No effect of orientation was observed.

## 3. Materials

The manufacturer's reported property data for non-irradiated grade NBG-10 are given in Table 1 [2,3]. SGL provided ORNL with a slab of NBG-10 graphite cut from billet No. 348 (green batch No. 1431) [3]. The original billet, as manufactured, measured $52 \times 26 \times 123$ cm and the slab provided to ORNL had dimensions of $52 \times 13 \times 47$ cm. Fig. 1 shows the orientation of the slab with respect to the original billet and the forming direction. The slab cutting plan for the ORNL slab is shown in Fig. 2.

Each of the four blocks shown in Fig. 2 was divided along its major axis to yield four 'PARA' slices and four 'PERP' slices. Specimens were then machined with their major axis parallel to the extrusion direction from the 'PARA' slices, i.e., with grain, WG (Fig. 3) and perpendicular to the

Table 1
Manufacturer's physical property data for NBG-10

| Property | Skin | Core |
|---|---|---|
| Apparent density, g/cm$^3$ | 1.81 | 1.79 |
| Thermal conductivity (21 °C), W/m K | 161 (WG)<br>157 (AG) | 148 (WG)<br>145 (AG) |
| Electrical resistivity, μΩ m | 8.4 (WG)<br>8.6 (AG) | 9.1 (WG)<br>9.3 (AG) |
| Flexural strength (4 pt.), MPa | 30 (WG)<br>27 (AG) | 24 (WG)<br>27 (AG) |
| Tensile strength, MPa | 18 (WG)<br>21 (AG) | 20 (WG)<br>18 (AG) |
| Compressive strength, MPa | 70 (WG)<br>60 (AG) | 47 (WG)<br>61 (AG) |
| Young's modulus, GPa | 10.3 (WG)<br>9.9 (AG) | 9.7 (WG)<br>9.7 (AG) |
| Coefficient of thermal expansion [20–200 °C], $10^{-6}$ °C$^{-1}$ | 4.2 (WG)<br>4.3 (AG) | 4.1 (WG)<br>4.6 (AG) |
| Isotropy ratio ($\alpha_{AG}/\alpha_{WG}$) | 1.02 | 1.12 |
| Ash content, ppm | 140 | 140 |

WG = with the grain: AG = against the grain.

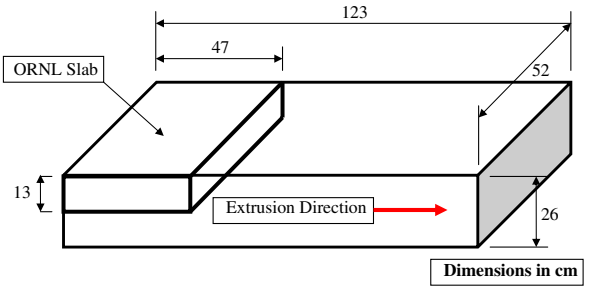


Fig. 1. Schematic diagram of NBG-10 billet No. 348 indicating the location of the slab provided to ORNL for irradiation experiments, and the extrusion direction.

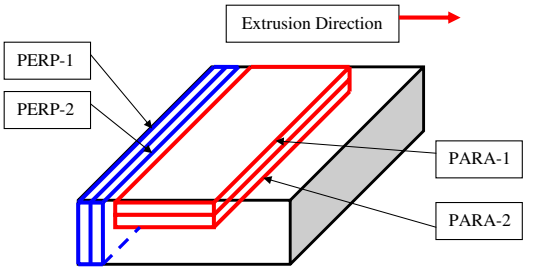


Fig. 2. Slab cutting diagram for the NBG-10 slab provided to ORNL.

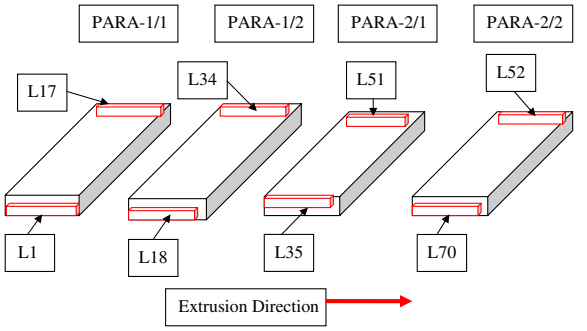


Fig. 3. Specimen cutting plan for the parallel to extrusion NBG-10 specimens.

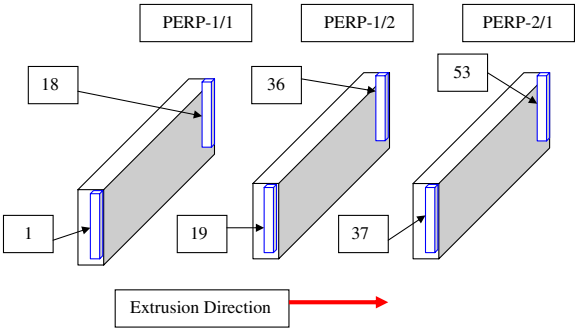


Fig. 4. Specimen cutting plan for perpendicular to extrusion NBG-10 specimens.

extrusion axis from the 'PERP' slices, i.e., against grain, AG (Fig. 4). A total of 70 PARA specimens were machined from slices PARA-1/2, -1/2, -2/1 and -2/2 (Fig. 3) and were identified as specimens L1 through L70. Slice PERP-2/2 was not used and a total of 53 PERP specimens were machined from slices PERP-1/1, -1/2, and -2/1 (Fig. 4).

All of the NBG-10 specimens irradiated in this work were from the 'PARA' slabs (samples L1–L70) and thus had their major axis aligned parallel to the extrusion direction.

## 4. Results

Volume change data for NBG-10 at all three irradiation temperatures are reported in Fig. 5. The dimensional change data in the parallel or with-grain (WG) direction (specimen length direction) at irradiation temperatures of $294 \pm 25$, $360 \pm 25$ and $691 \pm 25$ °C are given in Fig. 6. The dimensional changes in the perpendicular (against-grain, AG) direction are reported in Fig. 7 (specimen width direction) and in Fig. 8 (specimen thickness

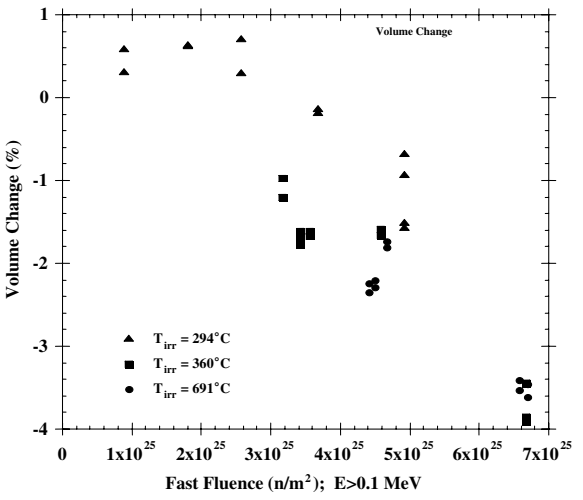


Fig. 5. Volume change behavior of NBG-10 graphite.

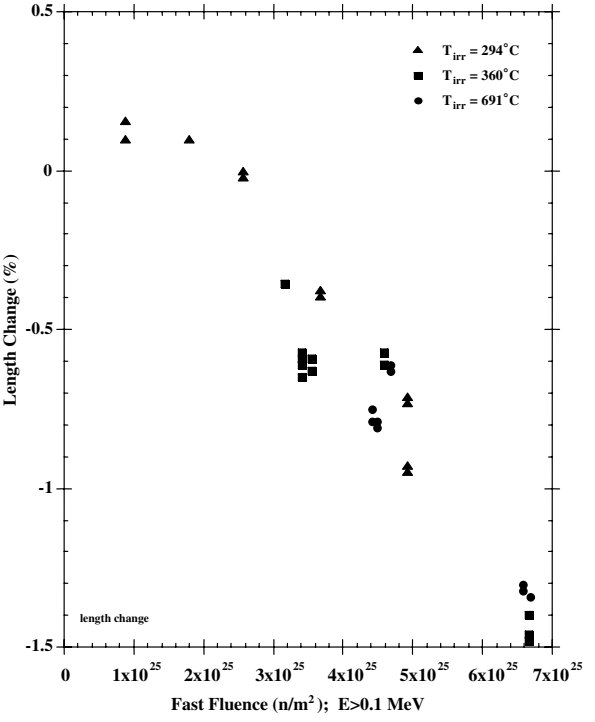


Fig. 6. Dimensional change behavior in the parallel to extrusion or specimen length direction for NBG-10 graphite.

direction). The volume and dimensional change data reported here are plotted without error bars. The errors associated with dimensional measurements are small, typically <0.1%. Capsule dosimetry calculations are based on HFIR flux maps made using a variety of flux wires over many years of

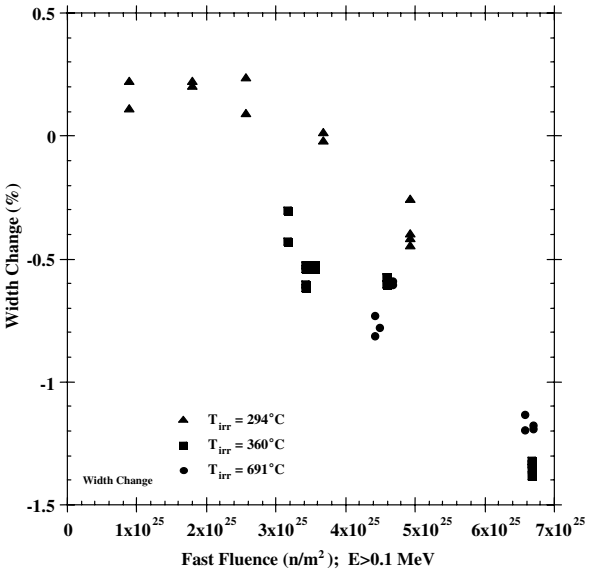


Fig. 7. Dimensional change behavior in the perpendicular to extrusion or specimen width direction for NBG-10 graphite.

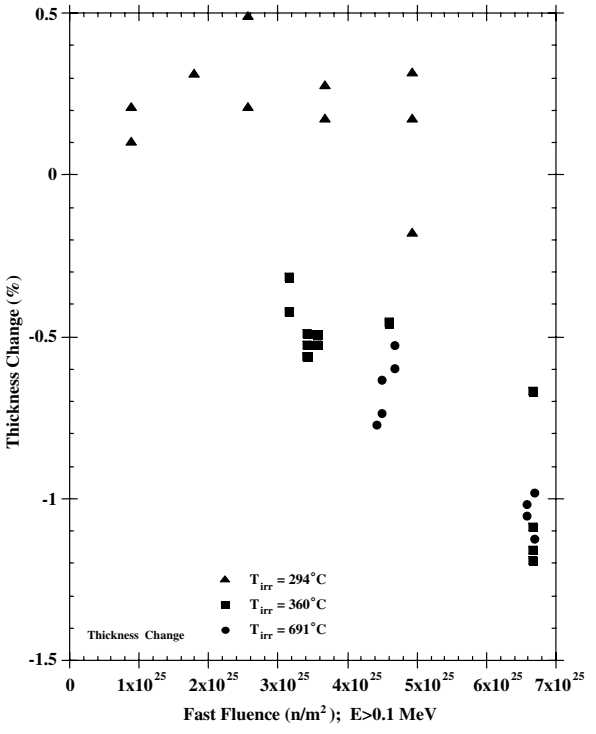


Fig. 8. Dimensional change behavior in the perpendicular to extrusion or specimen thickness direction for NBG-10 graphite.

HFIR operation. Potential errors associated with dosimetry estimates are typically $<\pm 5\%$. The greatest sources of potential errors in the reported data are the uncertainties associated with the exact specimen irradiation temperatures. The SiC temperature monitors were read using an isochronal annealing and electrical resistivity technique as described elsewhere [1]. The measured irradiation temperatures were $294 \pm 25$, $360 \pm 25$ and $691 \pm 25$ °C. The estimated measurement error of ±25 °C on the irradiation temperature represents an error of $<\pm 10\%$.

Room temperature bend strength was determined for non-irradiated graphite using a population of 22 samples. It was determined that the most appropriate analytical description of the failure for the non-irradiated bend bars was a Weibull treatment. For the 22 test strengths the Weibull modulus was 11.56 and the shape parameter 24.71 MPa, yielding a Weibull mean of $23.65 \pm 5.02$ MPa. However, given the small number of samples at the irradiation condition comparison using normal statistics is more practical. The mean using normal statistics $23.64 \pm 2.6$ MPa (one standard error) is practically identical to the Weibull mean. The use of normal statistics is therefore considered appropriate and applied from here forward.

## 5. Discussion

### 5.1. Displacement damage

Radiation damage in graphite occurs when energetic particles, such as fast neutrons, impinge on the crystal lattice and displace carbon atoms from their equilibrium positions – creating a lattice vacancy and an interstitial carbon atom. The displaced carbon atoms recoil through the lattice and produce other carbon atom displacements in a cascade effect. The cascade carbon atoms tend to be clustered in small groups of 5–10 atoms and it is generally satisfactory to treat the displacements as if they occur randomly. However, not all of the carbon atoms remain displaced. The displaced carbon atoms diffuse between the graphite layer planes in two dimensions and a high proportion of them will recombine with lattice vacancies. Others will coalesce to form linear molecules, which in turn may form the nucleus of a dislocation loop – essentially a new graphite plane. Interstitial clusters, on further irradiation, may be destroyed by impinging neutrons or energetic displaced carbon atoms (irradiation annealing). Adjacent lattice vacancies in the same graphite crystal basal plane are believed to collapse parallel to the basal plane, thereby forming sinks for other vacancies that are increasingly mobile above

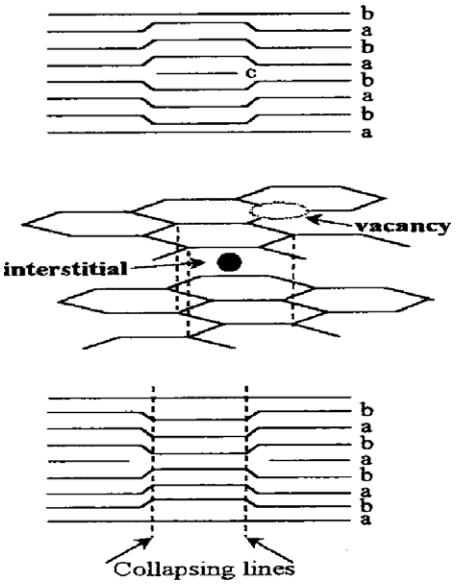


Fig. 9. Displacement damage mechanism in graphite.

600 °C, and hence can no longer recombine and annihilate interstitials. This mechanism is illustrated in Fig. 9. The lattice strain that results from displacement damage causes significant structural and property changes in the graphite.

### 5.2. Mechanism of dimensional change behavior

A principal result of the carbon atom displacements discussed above is crystalline dimensional change. Interstitial defects will cause crystallite growth perpendicular to the layer planes (*c*-axis direction), whereas coalescence of vacancies will cause a shrinkage parallel to the layer planes (*a*-axis direction). The damage mechanism and associated dimensional changes are illustrated in Fig. 10.

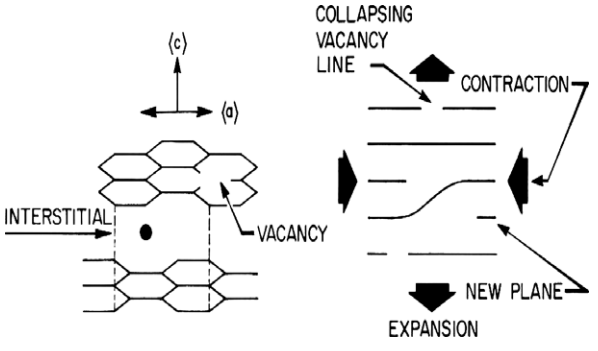


Fig. 10. Neutron irradiation damage mechanism in graphite showing the induced crystal dimensional changes.

Polygranular graphite exhibits a polycrystalline structure, usually with significant texture resulting from the method of forming during manufacture. Consequently, structural and dimensional changes in polygranular graphite are a function of the crystallites dimensional change and the graphite's texture. In polygranular graphite, thermal shrinkage cracks (formed during manufacture) that are preferentially aligned in the crystallographic *a*-direction initially accommodate the *c*-direction expansion, so mainly *a*-direction contraction is observed. Hence, the graphite undergoes net volume shrinkage. This behavior is illustrated with data from grade H-451 graphite, an extruded grade used in the Fort St. Vrain HTGR. As seen in Fig. 11, H-451 exhibits volume shrinkage behavior at irradiation temperatures of 600 and 900 °C. With increasing neutron dose (displacements), the incompatibility of crystallite dimensional changes leads to the generation of new porosity, and the volume shrinkage rate falls, eventually reaching zero. The graphite then begins to swell at an increasing rate with increasing neutron dose because of the combined effect of *c*-axis growth and new pore generation. The graphite thus undergoes a volume change 'turnaround' into net growth which continues until the generation of cracks and pores in the graphite, due to differential crystal strain, eventually causes total disintegration of the graphite (Fig. 11).

At low irradiation temperatures, typically <300 °C, volume growth may be observed initially, followed by the rapid onset of volume shrinkage [4,5]. The low dose volume swelling has been attributed to the relaxation of fabrication stresses [5,6]. With increasing dose the volume shrinkage behavior would be expected to turnaround to net swelling [7].

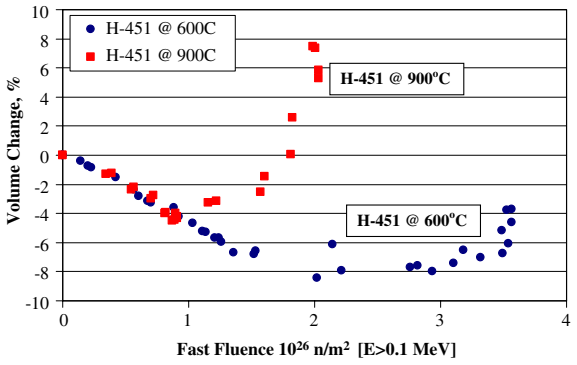


Fig. 11. Irradiation-induced volume changes for H-451 graphite at two irradiation temperatures ([8]).

H-451 graphite is an extruded material and thus the filler coke particles are preferentially aligned in the extrusion axis (parallel direction). Consequently, the crystallographic *a*-direction is preferentially aligned in the parallel direction and the *a*-direction shrinkage is more apparent in the parallel (to extrusion) direction, as indicated by the parallel direction dimensional change data in Figs. 12 and 13. The dimensional and volume changes are greater at an irradiation temperature of 600 °C than at 900 °C, i.e., both the maximum shrinkage and the turnaround dose is greater at an irradiation temperature of 600 °C. This temperature effect can be attributed to the thermal closure of internal porosity aligned parallel to the *a*-direction that accommodates the *c*-direction swelling. At higher irradiation temperatures a greater fraction of this accommodating porosity is closed and thus the shrinkage is less at the point of turnaround.

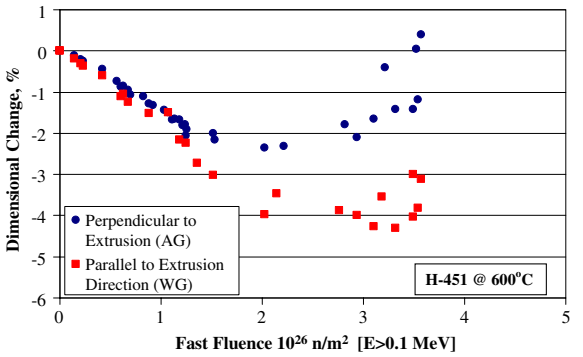


Fig. 12. Dimensional change behavior of H-451 graphite at an irradiation temperature of 600 °C ([8]).

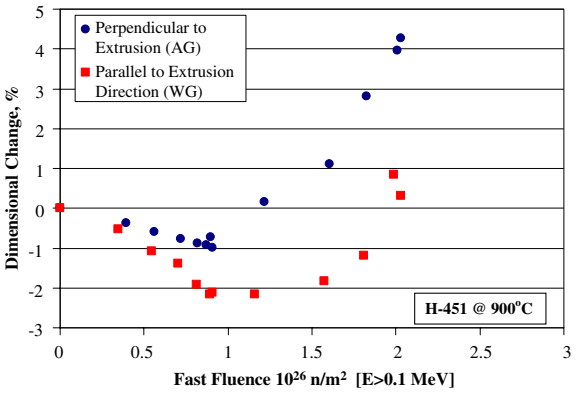


Fig. 13. Dimensional change behavior of H-451 graphite at an irradiation temperature of 900 °C ([8]).

The irradiation induced dimensional change behavior of grade NBG-10 is now discussed in light of the mechanisms reviewed above and compared to that of H-451 graphite.

### 5.3. Low temperature dimensional changes of NBG-10 graphite

Low temperature volume change behavior of NBG-10 is shown in Fig. 5. The graphite initially swells, the rate of swelling falls with increasing dose followed by a reversal to shrinkage. The low temperature (~300 °C) dimensional changes of NBG-10 are shown in Figs. 6–8 and are compiled in Fig. 14. The dimensional change data in the specimen thickness direction (perpendicular to extrusion) should be treated with some caution because of the small dimension of the specimen (~2.85 mm) in comparison with the maximum grain size of the graphite (1.6 mm) [2]. NBG-10 is seen to expand in both the parallel (WG) and perpendicular (AG) directions at low doses, followed by a turnaround (reversal) to shrinkage at higher doses. The maximum swelling is ~0.16% in the parallel direction and 0.2–0.3% in the perpendicular direction.

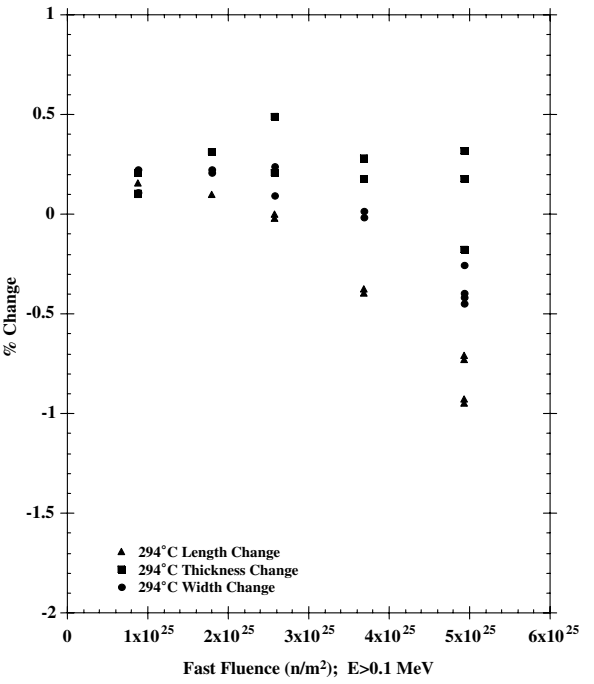


Fig. 14. Low temperature dimensional change behavior of NBG-10 graphite.

The dimensional changes of NBG-10 graphite at low temperature (<300 °C) in the perpendicular or AG direction (specimen width and thickness) are typical of that for extruded graphites. As reviewed by Simmons [4], pile grade A (PGA) graphite (used as the moderator in the UK Magnox reactors) exhibits temperature dependant swelling at low temperatures in the against-grain (perpendicular) direction. The magnitude of the swelling is dose and temperature dependant, exceeding several percent at 150 °C. At 250 °C and a dose of $3 \times 10^{21}$ n/cm$^2$ the swelling was ~0.3%. Nightingale [5] reports the behavior of CSF graphite at irradiation temperatures in the range 30–340 °C at low doses. These data show strong temperature dependence in the magnitude of the against-grain (perpendicular) swelling behavior. Nightingale [5] also reviews higher dose studies of several graphites, including grades KC, CSGBF, and Spear, irradiated at temperatures in the range 400–500 °C. Significantly, the graphites all exhibit swelling in the parallel (WG) direction as well as in the perpendicular (AG) direction. However, the magnitude of the swelling was small because of the higher irradiation temperature. This swelling behavior was attributed to the relaxation (irradiation creep) of internal residual stresses at low doses. These residual stresses arise during manufacture and/or are induced by specimen machining. Indeed, Kennedy and Woodruff [6] incorporated a stress relaxation term in their dimensional change model of grade TSX graphite.

In a study of PGA graphite from irradiation specimens withdrawn from operating commercial Magnox reactors, Burchell and Wickham [7] report the irradiation induced dimensional change behavior over the temperature range 210–400 °C. In the perpendicular direction, an initial swelling was observed at all temperatures studied, followed by reversal into shrinkage. In the temperature range 220–230 °C (Calder equivalent temperature), the maximum swelling was ~0.1% with a return to original volume at a dose of $1.1 \times 10^{21}$ n/cm$^2$ (EDN) or $2.2 \times 10^{21}$ n/cm$^2$ [$E > 0.1$ MeV].

In general the low temperature behavior of NBG-10 is similar to that observed in other extruded graphites. The magnitude of the swelling is perhaps somewhat larger than previously reported. It should be noted that the anisotropy ratio of NBG-10 is much smaller than the older extruded grades mentioned here. Consequently, the differenced between AG and WG dimensional changes should be less striking in the case of NBG-10. Furthermore, the initial growth and turnaround to shrinkage at lower temperature, which is typically attributed to the relaxation of residual stresses, may be more significant in this work due to relatively small dimensions of the specimen compared to the graphite's maximum grain size.

### 5.4. High temperature dimensional changes of NBG-10 graphite

The volume change behavior of NBG-10 graphite is shown in Fig. 5. The 360 and 691 °C volume changes are very similar in magnitude and dose dependency at lower dose, exhibiting volume shrinkage at an increasing rate with dose. At higher doses there is evidence for a divergence of the data, as would be expected. At the doses reported here there is no evidence for the onset of turn-around into volume growth. The volume change behavior exhibited at high temperatures (~700 °C) by NBG-10 is similar to that seen for grade H-451 graphite (Fig. 11) [8]. In H-451 the onset of turnaround begins at $\sim 1 \times 10^{26}$ n/m$^2$ at 900 °C and $\sim 2.5 \times 10^{26}$ n/m$^2$ at 600 °C. Moreover, for H-451, the volume shrinkage rates at 600 and 900 °C are similar. A comparison of Figs. 5 and 11 indicates NBG-10 exhibited ~3.5 vol.% shrinkage at a dose of $6.7 \times 10^{25}$ n/cm$^2$ compared to 3–4 vol.% at a similar dose for H-451.

The high temperature dimensional change behavior of NBG-10 graphite is shown in Figs. 6–8. The behavior at 691 °C in the perpendicular (width and thickness) and parallel (length) directions is shown in Fig. 15. Anisotropy in the dimensional change is evident from the data in Fig. 15, as would be expected for extruded graphite. The shrinkage for a given dose is greater in the parallel (WG) or length direction than in either of the perpendicular (AG) directions (width and thickness directions). As discussed previously, this anisotropy can be attributed to the preferential alignment of the filler particle in the direction of extrusion, thus tending to preferentially align the $\langle a \rangle$ axis in the extrusion (WG) direction. The WG (length direction) behavior is thus more heavily influenced by the $\langle a \rangle$ axis shrinkage than the AG direction. At the fluences reported here, NBG-10 does not show any sign of turnaround into swelling at either 360 or 691 °C. At 691 °C there is slight anisotropy in the dimensional change behavior of NBG-10, the WG direction exhibiting slightly more shrinkage than the AG directions. Moreover, the magnitude of the

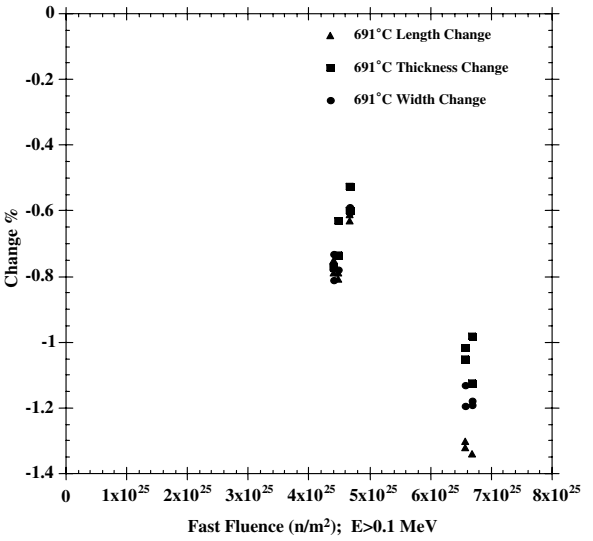


Fig. 15. High temperature dimensional change behavior of NBG-10 graphite.

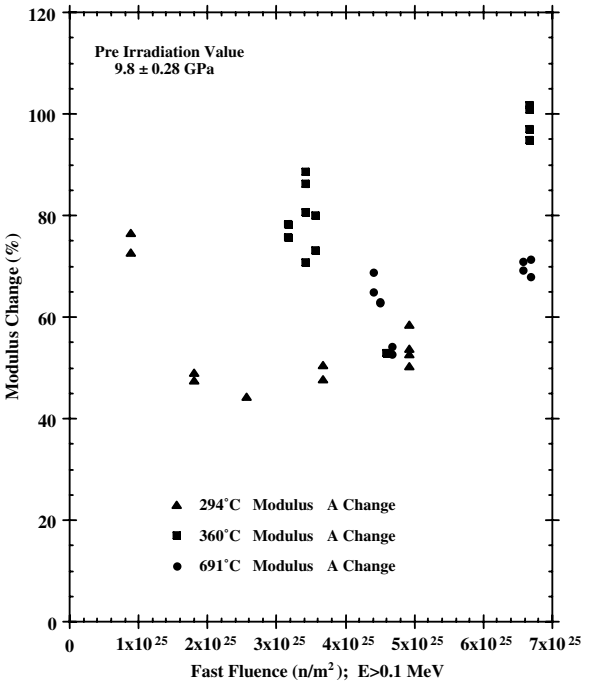


Fig. 16. The variation of dynamic Young's modulus with dose for NBG-10 graphite.

shrinkages in NBG-10 at 710 °C and $6.7 \times 10^{25}$ n/cm$^2$ [$E > 0.1$ MeV] were comparable to that exhibited by H-451 at a similar fluence and an irradiation temperature of 600 °C.

### 5.5. Strength and modulus changes

As discussed in Section 4.1, significant property changes occur during neutron irradiation. Imperfections in the crystal structure, such as interstitial atoms and basal plane vacancies act as dislocation pinning sites causing an increase in the elastic constants and strength. Moreover, changes in the pore structure resulting from the anisotropic crystal dimensional changes will additionally affect the strength and elastic constants. Pore closure due to $\langle c \rangle$ axis expansion will cause a gradual increase in strength and elastic constants, whereas the subsequent generation of new porosity due to the incompatibility of crystal strains at higher doses causes a reduction in strength and modulus, and the eventual disintegration of the graphite.

Fig. 16 shows the variation of dynamic modulus with dose for all of the NBG-10 irradiation samples. At higher temperatures (>300 °C) the modulus increases with dose as expected, under the influence of irradiation induced defects that inhibit basal plane dislocation mobility. At the doses reported here, and at the higher irradiation temperatures, only modulus increase would be anticipated since the graphite remains in volume shrinkage (Fig. 5). The low temperature (and low dose) modulus behavior is more complex. As previously discussed, the graphite initially swells due to the relaxation (creep) of internal stresses (arising from manufacture and machining) prior to the onset of volume shrinkage. Thus, the 294 °C behavior is a combination of reducing internal stress, increasing defect concentration, and pore closure. Note also that basal plane vacancies are relatively immobile at this temperature and thus the concentration of defects will be greater at a given dose than for the higher temperature irradiations.

Fig. 17 shows the NBG-10 graphite elastic modulus data and compares them with H-451 data taken at 600 and 900 °C. Note that the H-451 modulus is measured by the sonic velocity method and not the resonant frequency technique employed here for the NBG-10. Thus small differences might be expected. However, as shown in Fig. 17, the H-451 and NBG-10 modulus data are quite similar.

The effects of irradiation dose on the flexure strength of NBG-10 graphite are shown in Fig. 18 for all three experimental irradiation temperatures. The effect of irradiation temperature on the bend strength of the NBG-10 graphite is less clear than the other properties studied. This is probably due

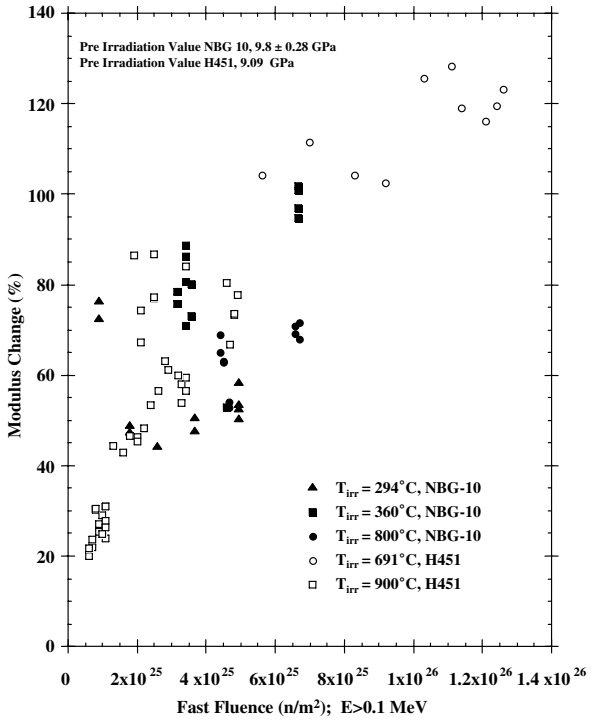


Fig. 17. A comparison of the variation of dynamic Young's modulus with dose for NBG-10 and H-451 graphite.

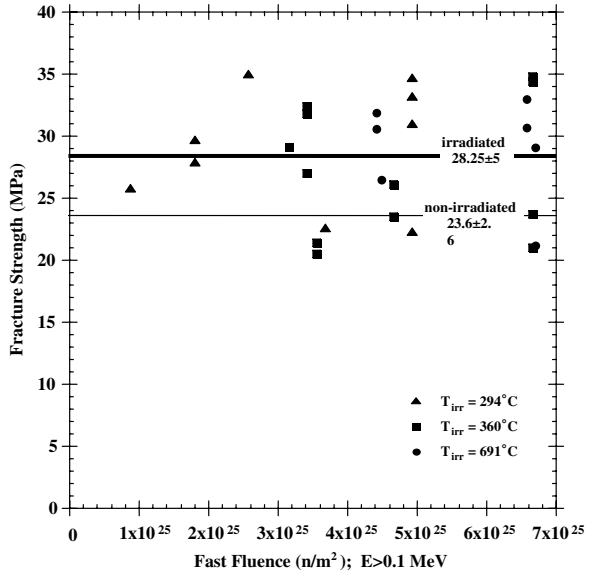


Fig. 18. The variation of 4-pt flexure strength with dose for NBG-10 graphite.

to the statistical limitation of the irradiation experiment, and the small thickness of the specimen compared to the NBG-10 grain size. However, it can be concluded that there is a strengthening of the graphite on irradiation. As shown in Fig. 18, if all irradiated strength data are averaged, the mean strength is $28.25 \pm 5$ MPa, or a 20% increase over the non-irradiated strength. Pooling the samples according to temperature (regardless of fluence) yields strength increases of 23% at 294 °C, 16% at 360 °C, and 18% at 691 °C. Such increases in strength are expected for the reasons discussed above.

## 6. Conclusions

Thirty-six NBG-10 graphite flexure bars have been successfully irradiated in a series of 18 HFIR PTT capsules at ORNL. The peak doses attained were 4.93, 6.67 and $6.69 \times 10^{25}$ n/m$^2$ [$E > 0.1$ MeV] at irradiation temperatures of ~294, ~360 and ~691 °C (±25 °C), respectively.

The high temperature irradiation volume and dimensional change behavior of NBG-10 were similar to other extruded near isotropic grades, such as H-451, which has been irradiated previously at ORNL. The low temperature (~300 °C) behavior was also as expected for extruded graphites, i.e., exhibiting low dose swelling prior to shrinkage. This behavior was attributed to the relaxation of internal stress arising from the graphite manufacturing process and specimen machining.

The elastic modulus and flexure strength of the graphite increased over the dose range examined here, as expected from prior studies. Large scatter in the strength data was observed due to the small dimensions of the PTT capsule specimen compared to the maximum grain size of NBG-10 graphite.

While the data reported here do not represent a complete database for NBG-10 graphite, they give a measure of confidence that the current generation of nuclear graphites will behave in a familiar and well understood manner.

## Acknowledgement

This work is sponsored by the US Department of Energy, Office of Nuclear Energy Science and Technology under Contract DE-AC05-00OR22725 with Oak Ridge National Laboratory, managed by UT-Battelle, LLC.

## References

[1] L.L. Snead, A.M. Williams, A.L. Qualls, Revisiting the use of SiC as a post irradiation temperature monitor, in: Proceeding

of the Effects of Radiation on Materials: 21st International Symposium, ASTM International, West Conshohocken, PA, p. 2004.
[2] B. Tahon, F. Gerstgrasser, Nuclear Graphite Grades presented at the Generation IV Reactors International Forum, Knutsford, Cheshire, UK, 7 September 2004.
[3] B. Tahon, Personal Communication, 2005.
[4] J.W.H. Simmons, Radiation Damage in Graphite, Pergamon, New York, London, 1965.
[5] R.E. Nightingale, Nuclear Graphite, Academic Press, 1962.
[6] C.R. Kennedy, E.M. Woodruff, Irradiation Effects on the Physical Properties of Grade TSX Graphite, Westinghouse Hanford Company, Richland, Washington, 1989.
[7] T.D. Burchell, A.J. Wickham, The dimensional change in pile grade A graphite irradiated in CEGB magnox power reactors, in: Proceedings of 18th CARBON '87, 18th Biennial Conference on the Carbon, 1987.
[8] T.D. Burchell, in: Proceedings of the CARBON '02, 15–19 September 2002. Beijing, China, 2002.